RESPONSES OF THE SCALED INFANT HUMAN BODY MODEL IN SIMULATED FRONTAL MOTOR VEHICLE CRASHES

Sophia Tushak
Center for Injury Research and Prevention, The Children's Hospital of Philadelphia
Joint Department of Biomedical Engineering, UNC-Chapel Hill/NC State University
United States

Jalaj Maheshwari
Aditya Belwadi
Center for Injury Research and Prevention, The Children's Hospital of Philadelphia
United States

Paper Number 19-0142

ABSTRACT

Most motor vehicle crash deaths occur among children traveling as passenger vehicle occupants, and proper restraint use and direction of use can reduce these fatalities. There is little to no literature on systematic evaluation on the responses of children under three-years of age in motor vehicle crashes. The study presents the first ever endeavor at developing 18MO, 24MO, 30MO, and 36MO pediatric finite element models from the 6YO PIPER human body model as the baseline and comparing their responses in rear-facing and forward-facing simulations of the same crash pulse conditions in the FMVSS No. 213 test bench and a vehicle seat.

The 6YO PIPER model was scaled down to create anthropometrically accurate models of the 18MO, 24MO, 30MO and 36MO child using the PIPER scaling tool and Snyder anthropometric data. Each model (N=4), along with a convertible car seat and either the 213-test bench or a 2012 Toyota Camry vehicle rear seat was simulated in a full-frontal crash (24G, 120ms pulse). Kinetics and kinematics were extracted and processed as per SAEJ211 metrics.

On the 213-test bench, models in forward-facing configuration showed higher head accelerations, but lower pelvis accelerations for 30MO and 36MO models. Chest displacements were between 84-90% higher in the forward-facing models, with the exception of the 30MO model, which was 35% higher. Neck moments were lower in all rear-facing configurations. Upper neck forces were at least six times higher forward-facing. HIC36 in rear-facing models ranged from 300-344, while HIC36 in forward-facing models ranged from 410-494, showing no linear trend as age increased. Forward-facing head excursions grew over two-fold from their rear-facing counterparts, from an average of 240 to an average of 518. Head trajectories generally followed a longer path in forward-facing models. NIJ for all forward-facing models were five to eight times the values for rear-facing. On the vehicle seat, the forward-facing models showed higher head accelerations for 24MO and 36MO models. Chest displacements were 33-49% higher in forward-facing models, except 36MO, where it was 128% higher. Neck forces and moments were consistently lower for rear-facing models as compared to forward-facing. Upper neck forces were 6.5-9.75 times higher in forward-facing models. HIC36 values were lower in rear-facing, ranging from 335-394, as compared to forward-facing which were 455-624. Head excursions for forward-facing were three times that for rear-facing, except the 36MO model, where it was 1.75 times higher. NIJ for all forward-facing models were six to nine times the values of rear-facing.

Kinetics and kinematics numbers across the board were within IARV limits. Pediatric models in rear-facing configurations generally had lower injury numbers than those in frontal configurations. However, there is no consistent trend seen in injury values as age progresses. This is the first study to conduct a systematic evaluation of the response of children under three years old in frontal motor vehicle crashes.

INTRODUCTION

Motor vehicle crashes (MVCs) are the leading cause of death among children over the age of one [1]. Most knowledge about pediatric injury rates is derived from real-world crash databases, sled testing via anthropometric test devices (ATDs) aged from newborn to 10 years old, and post-mortem human subjects (PMHS), but little has been investigated using computational finite element (FE) analysis and human body models (HBMs) to predict the occurrence of potential injuries in unique crash conditions. Misuse of child restraint systems (CRSs) is a prevalent problem when transporting children. Misuse rates are typically generated from observational studies and vary depending on the sample population included in the analysis. The implications of CRS misuse on injury risk should be assessed using a systematic approach that reduces the number of confounding variables to determine specific injuries associated with misuse.

Current Methods to Assess Injury in Children

Field Databases Despite the gravity of the problem, most of the current knowledge on pediatric injuries from MVCs is obtained from fatal crash reports, and minimal efforts have been made to examine non-fatal crash statistics [2]. Field data can be vague and confusing since the crash reports have many confounding variables, such as the region of the country in which the accident occurred, subject age, car model, impact speed, and crash mode.

Post-Mortem Human Subjects The use of PMHS is common in biomechanical and anatomical assessments of adult populations, but their usage in pediatric populations is far more scarce due to the infrequency of available specimens. The lack of comparable data causes large gaps in knowledge of pediatric injury risk as well as inaccuracies when developing other methods for assessing injury risk, such as ATDs and FE human body models (HBMs).

Anthropometric Test Devices Child ATDs have been used for several decades to study whole-body responses in MVCs. While their biofidelity has improved, they lack the same capacity for anatomical specificity and tissue-level kinematic and kinetic responses as PMHS. Additionally, ATD whole-body responses are only validated for impacts in one direction (frontal, lateral, rear), so their injury outcomes are restrictive to one crash mode.

Finite Element Analysis The newest method of assessing injury in MVCs is FE analysis, which offers a customizable, low-cost, and repeatable computational means to represent the variations due to age and size in different populations [3]. Due to the scarcity of pediatric PMHS and the subjective nature of field data, FE analysis poses an excellent alternative. However, FE responses are based on how the model is defined, so if the model is inaccurate, the responses cannot be trusted. Many existing FE ATD models and HBMs are derived by scaling down adult geometry to child geometry, but this is inappropriate since anthropometric and anatomical differences exist between the two populations [4], namely in the head [5], neck [6], torso [7], and pelvis [8]. The PIPER 6YO Child model is one of the only HBMs developed and validated from child PMHS data. Other similar HBMs, including Wayne State University's CHARM-10 10-year-old model and the Global Human Body Models Consortium's (GHBMC) 6-year-old model, were developed from child PMHS data but are pedestrian models rather than occupant models. Along with the release of the pediatric model, the PIPER project released the PIPER software, a program that continuously scales and quickly positions FE models. This new pediatric HBM and useful program create the potential to accurately predict injuries in children of all ages and sizes in multidirectional impacts.

Misuse of Child Restraint Systems

Previous studies have uncovered a 63-90% CRS misuse rate with at least one installation error [9-14]. Misuse errors vary, and some errors are more detrimental than others. However, the cumulative effect of several small errors can result in the effect of one large error [15-20]. The rear-facing configuration is safest for infants since the CRS protects the anterior loading of the head, neck, torso, and pelvis in the event of a frontal impact car crash by evenly distributing the load across the back face of the CRS and reducing neck flexion, head acceleration, and chest displacement [21]. A convertible CRS allows for effortless transition from rear-facing to forward-facing configurations, but is usually limited to infants under 18 kg. Countries have different recommendations for how long children should remain in rear-facing CRSs. For example, the United States suggests that parents refrain from switching their children to forward-facing until at least the age of 2 years old. Sweden, however, suggests that parents wait until children reach five years old to make the switch. A potentially premature transition may have

severe consequences and could lead to injurious loading or ejection if the belt path is not in the proper orientation for that configuration [21]. A study by Henary et al [22] found a 5.5 times and 1.2 times greater injury risk during side and frontal impacts, respectively, for children under the age of two in forward-facing CRSs. Spinal cord injuries are among the most notable since children's heads are disproportionate in relation to the rest of their body, causing greater head rotation and tensile loads to the cervical spine [21].

Installation angle of rear-facing CRSs is vital. A CRS that is too erect may inhibit breathing if the infant's head is tipped forward. A CRS that is too reclined causes the upward projected force to surpass the reaction force of the back of the CRS, thereby ineffectively restraining the infant. Car seat manufacturers generally suggest a 30 to 45 degree recline angle of the back of the CRS with respect to the vertical axis. For a larger infant, a 30 degree recline may be more appropriate to ensure better crash protection. For a smaller infant, a 45 degree recline is better to allow for ample crash protection, but also discourage the head from leaning too far forward and potentially impairing breathing [21]. Understanding the implications of CRS misuse can provide education for parents as to how severe the consequences of improper installation may be.

Study Goals

Little to no literature on the systematic evaluation of the kinematic and kinetic responses of children under three years of age in MVCs exists. This study presents the first ever endeavor at developing 18MO, 24MO, 30MO, and 36MO pediatric finite element models from the 6YO PIPER HBM and comparing their responses in rear-facing and forward-facing simulations of the same crash pulse conditions in the Federal Motor Vehicle Safety Standards (FMVSS) No. 213 test bench and a 2012 Toyota Camry vehicle seat.

METHODS

The 6YO PIPER Child model was scaled down to create anthropometrically accurate models of the 50th percentile 18MO, 24MO, 30MO and 36MO child using the PIPER scaling tool and Snyder anthropometric data [23]. Each model (N=4), along with a convertible car seat (rear-facing and forward-facing configurations) and either the FMVSS No. 213 test bench or a 2012 Toyota Camry vehicle rear seat was simulated in a full-frontal crash (24G, 120ms pulse) using LS-DYNA (v.971_R8, Livermore Software Technology Company, Livermore, CA) for a total of 16 simulations. Kinetics and kinematics were extracted and processed as per the Society of Automobile Engineers (SAE) J-211 metrics.

Age-Based Scaling

The PIPER 6YO Child model was scaled using the PIPER software (v1.0.1). The 6YO child model was imported into the PIPER program and scaled to 18 month-old (18MO, m=12.6 kg), 24 month-old (24 MO, m=13.7 kg), 30 month-old (30MO, m=14.8 kg), and 36 month-old (36 MO, m=16.0 kg) 50th percentile models. When scaling, one landmark was missing from the thoracic spine, causing a mesh deformity in the upper thoracic spine (Fig.1A). To fix this, the missing landmark was added to the target file in NotePad++ before scaling again in PIPER, without causing a deformity in the mesh (Fig. 1B). The scaled models were exported to be used in finite element (FE) simulations.

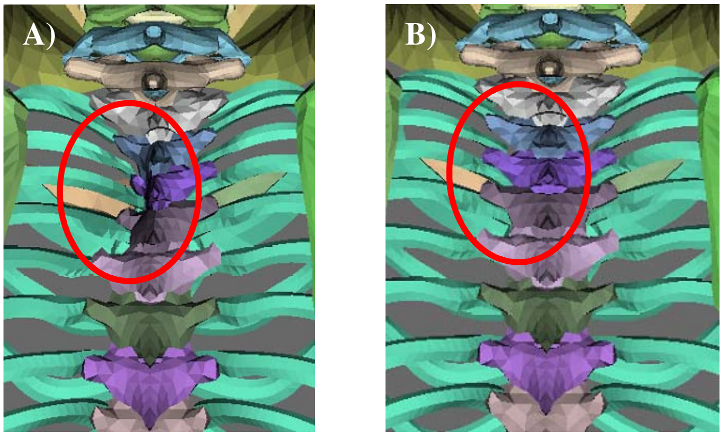

Figure 1. A missing landmark A) causes a deformity in the upper thoracic spine after scaling, B) but was later fixed.

Seat Preparation

A FE model of a convertible car seat (polypropylene plastic: E=10 GPa, $\rho=9e^{-7}$ kg/m^3, $\nu=0.43$, m=8.0 kg) was developed from CAD data in HyperMesh (v.14.0, Altair HyperWorks, Troy, MI). FE models of the convertible car seat and either the FMVSS No. 213 test bench (steel: E=210 GPa, $\rho=6e^{-6}$ kg/m^3, $\nu=0.33$) or a 2012 Toyota Camry rear vehicle seat (plastic: E=1.0 GPa, $\rho=7.11e^{-7}$ kg/m^3, $\nu=0.30$ and foam: E=0.00416 GPa, $\rho=1.01e^{-7}$ kg/m^3, m=6.9 kg) were imported into HyperMesh. The car seat was positioned as close to the bench or seat without contacting it in both forward-facing and rear-facing configurations. The forward-facing car seat was kept at the default position, angled 23.5 degrees with respect to the vertical axis. The rear-facing car seat was rotated to 45 degrees with respect to the vertical axis, as suggested by the car seat manufacturer. The CRS was gravity-settled onto the test bench/Camry seat. All FE simulations were run in LS-Dyna on a 64-node double precision explicit solver. The combined car seat and base model was used in future simulations with the PIPER child models, resulting in models with the car seat and either the FMVSS No. 213 test bench or the Camry seat in forward-facing and rear-facing configurations.

Child Model Preparation

Each scaled PIPER child model (18MO, 24MO, 30MO, and 36MO) was positioned in PIPER. The hips, knees, and ankles were rotated by approximately 15, 20, and 10 degrees, respectively, so that the model could be positioned as close to the car seat as possible to reduce the time required to settle the model. Any mesh deformations accrued during the positioning process were smoothed in PIPER. Following that, the PIPER models were settled into the seat and base using the same method as in the seat preparation.

Simulated Frontal Vehicle Crashes

The settled models underwent seat belt routing. A buckle (steel: E=210 GPa, $\rho=6e^{-6}$ kg/m^3, $\nu=0.33$) was made with 2D elements and placed at the pelvis of the child model in an appropriate location. Using the HyperMesh belt routing tool, a five-point harness consisting of 2D shell elements with a width of 38 mm and 1D connecting elements was generated for each model, with two belts over the shoulders, two belts on the pelvic wings, and one belt between the legs (Fig. 2).

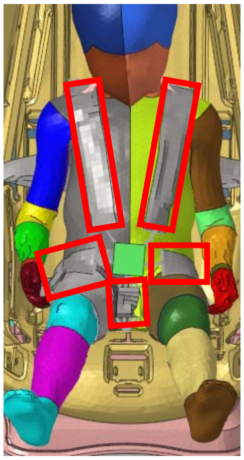

Figure 2. A 2D five-point harness was routed around each model and attached to a 2D buckle via 1D elements.

Once the model was secured in the car seat, the car seat was secured to the base. In the forward-facing configuration, a seat belt with a width of 48 mm was routed from the bottom anchor on the base, through the back of the car seat, and attached to the other bottom anchor on the base. Two additional seat belts were routed from the back anchor on the base, around the top of the base, and attached to the back of the car seat at the top anchor points (Fig. 3A-B). In the rear-facing configuration, a seat belt with a width of 48 mm was routed from the bottom anchor on the base, through the front of the car seat, and attached to the other bottom anchor on the base (Fig. 3C).

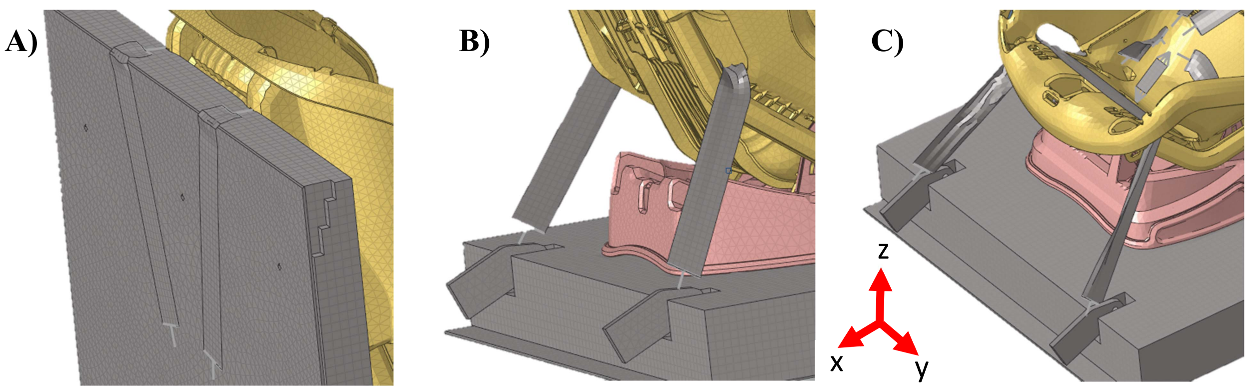

Figure 3. Seat belt routing of the CRS to the FMVSS No. 213 test bench. In the forward-facing configuration, seat belts were secured A) in two locations on the back of the test bench and B) to the two LATCH points on the bottom of the test bench. In the rear-facing configuration, a seat belt was secured C) to the two LATCH points on the bottom of the test bench. Since CRS manufacturers must be able to meet requirements without using a tether under the Federal Motor Vehicle Safety Standard (FMVSS) No. 213 test protocol, a top tether was not used. Similar belt routing was used for the Camry seat.

Model preparation with the Camry seat was set up identical to the 213-test bench, without a pretensioner, retractor, or load limiter. Surface-to-surface contacts were added for the interaction of the seat belt with the child model. Constant gravity was applied in the negative z-direction. The FMVSS No. 213 test pulse (24G) was applied to the base in the x-direction for a duration of 120 ms. Maximum head and pelvis accelerations, chest displacements, lower and upper neck forces and moments as well as head injury criteria (HIC), neck injury criteria (NIJ), and head excursions were extracted and processed as per the SAE J-211 metrics using LS-PrePost (v.4.5, Livermore Software Technology Company, Livermore, CA) and a custom MATLAB code (v.2017, MathWorks, Natick, MA).

RESULTS

Generally, the forward-facing model produced higher injury metrics than the rear-facing models (Table 1). On the FMVSS No. 213 test bench, head accelerations of the 18MO, 24MO, 30MO, and 36MO model in the forward-facing configuration were comparable to the rear-facing configuration, with 1.1-1.2 times (6.6%, 5.6%, 12.3%, and 19.0%, respectively) higher head accelerations. The opposite occurred for pelvis acceleration, where values were 1.1-1.2 times (18.4%, 12.3%, and 16.0%, respectively) higher in the rear-facing 18MO, 24MO, and 30MO models. The 36MO model did not continue this trend, with a pelvis acceleration 1.4 times (73.9%) greater in the forward-facing configuration. Maximum chest displacement ranged from 1.8-1.9 times (84.3-89.7%) higher in the forward-facing 18MO, 24MO, and 36MO models. Maximum chest displacement was substantially lower in the 30MO model, with a value of 1.3 times (34.8%) higher. Lower neck force varied greatly, with the 18MO model showing 0.8 times (17.7%) less force in the forward-facing configuration, the 24MO and 36MO models showing 1.5 and 1.4 times (48.2% and 38.7%) higher forces in the forward-facing configuration, respectively, and the 30MO model showing virtually no difference between the two seating arrangements. Considerably higher differences between forward-facing and rear-facing were seen in upper neck forces: the 18MO, 24MO, 30MO, and 36MO models were almost 15, 12, 7, and 8 times higher, respectively. Lower neck moments were all greater in the forward-facing configuration, with over 11-16 times greater moments. Upper neck moments, while still greater in forward-facing, did not show as great of a difference between seating arrangements (2.8, 3.4, 2.2, and 1.6 times higher for the 18MO, 24MO, 30MO, and 36MO models, respectively). HIC36 for the rear-facing models ranged from 302-344, but were much higher for the forward-facing models, which ranged from 409-494. Generally, the 18MO and 36MO models had higher HIC36 values than the 24MO and 30MO models. Nij ranged from 0.06-0.11 for the rear-facing models, and increased to 0.50-0.63 for the forward-facing models. Both rear-facing and forward-facing Nij were greatest in the 18MO model, lowest in the 24MO model, and similar for the 30MO and 36MO models. Head excursion was 3.4, 2.1, 2.6, and 1.4 times greater in the forward-facing configuration for the 18MO, 24MO, 30MO, and 36MO models, respectively. No correlations could be made between any metric and age of the model.

On the 2012 Toyota Camry seat, the 24MO and 36MO models in the forward-facing configurations showed 1.1-1.5 times (11.4% and 47.3%) higher head accelerations, respectively, while the 18MO and 30MO models showed 1.1 times (9.2% and 7.1%, respectively) higher head accelerations for rear-facing. Pelvis acceleration values were 1.0, 1.2, and 1.7 times (3.0%, 18.3%, and 72.9%) higher in the forward-facing 18MO, 30MO, and 36MO models, respectively. The 24MO model did not continue this trend, with a pelvis acceleration 2.3 times (73.9%) greater in the rear-facing configuration. Maximum chest displacement ranged from 1.3-1.5 times (33.3-48.8%) higher in the forward-facing 18MO, 24MO, and 30MO models. Maximum chest displacement was substantially higher in the 30MO model, with a value of 2.3 times (128.1%) higher. Lower neck force was 1.2-1.3 times (25.1%, 34.8%, and 23.7%, respectively) higher for the 18MO, 30MO, and 36MO models in the forward-facing configuration, and 1.8 times (81.1%) higher for the matched 24MO model. Considerably higher differences between forward-facing and rear-facing were seen in upper neck forces: the 18MO, 24MO, 30MO, and 36MO models were almost 9, 10, 10, and 7 times higher, respectively. Lower neck moments were all greater in the forward-facing configuration, with over 9-20 times greater moments. Upper neck moments, while still greater in forward-facing, did not show as great of a difference between seating arrangements (2.7, 5.0, 5.4, and 2.8 times higher for the 18MO, 24MO, 30MO, and 36MO models, respectively). HIC36 for the rear-facing models ranged from 336-383, but were much higher for the forward-facing models, which ranged from 455-624. HIC36 values varied greatly between models, with no similarities for any two models. Nij ranged from 0.06-0.11 for the rear-facing models, and increased to 0.54-0.64 for the forward-facing models. Both rear-facing and forward-facing Nij were greatest in the 36MO model and similar and lowest for the 24MO and 30MO models. Head excursion was 3.4, 3.3, 3.0, and 1.7 times greater in the forward-facing configuration for the 18MO, 24MO, 30MO, and 36MO models, respectively. No correlations could be made between any metric and age of the model.

Table 1.
Kinematic and kinetic responses of the 18MO (green), 24MO (blue), 30MO (orange), and 36MO (red) models during the simulated frontal crash.

	Max Head Acceleration (G)	Max Pelvis Acceleration (G)	Max Chest Displacement (mm)	Max Lower Neck Fz (N)	Max Lower Neck My (N*m)	Max Upper Neck Fz (N)	Max Upper Neck My (N*m)	HIC 36	Head Excursion	Nij
FF bench	63.2	53.4	30.5	561.0	8.9	1369.1	6.0	494.2	497.8	0.63
RF bench	59.3	65.5	16.5	681.8	0.7	91.6	2.1	306.1	144.6	0.08
FF Camry	58.2	79.4	26.0	828.9	9.0	1350.5	5.0	503.5	543.9	0.60
RF Camry	64.1	77.0	17.5	662.8	0.4	144.7	1.9	382.9	161.7	0.09
FF bench	54.3	53.3	22.9	783.8	10.0	1066.8	5.1	409.9	514.1	0.50
RF bench	51.4	60.8	12.3	528.8	0.9	90.6	1.5	343.1	239.6	0.06
FF Camry	58.7	52.8	18.5	849.4	10.5	1181.2	5.1	468.2	519.4	0.54
RF Camry	52.7	118.9	12.8	469.0	0.3	121.1	1.0	343.5	157.4	0.06
FF bench	64.0	44.0	22.1	746.8	10.2	1119.0	5.1	444.3	520.1	0.52
RF bench	57.0	52.4	16.4	751.7	0.8	165.9	2.3	344.4	200.0	0.11
FF Camry	55.5	62.6	20.6	792.7	9.8	1219.8	4.7	455.3	561.9	0.54
RF Camry	59.8	52.9	15.4	587.9	0.8	126.5	0.9	394.0	186.1	0.06
FF bench	60.9	64.9	27.0	707.1	11.4	1169.2	5.2	471.5	540.3	0.54
RF bench	51.2	45.9	14.3	509.8	0.7	156.9	3.2	302.2	373.6	0.11
FF Camry	71.7	64.1	31.0	844.4	11.4	1420.4	5.8	623.7	556.5	0.64
RF Camry	48.7	37.1	13.6	682.8	1.3	215.7	2.1	335.9	318.8	0.11

Differences between the test bench and Camry seat varied between seating configurations and ages. In the forward-facing configuration, the 18MO model and Camry seat showed an approximate 48% increase in maximum pelvis acceleration and lower neck force and 15% decrease in maximum chest displacement and upper neck moment. In the 24MO model, 10.7% and 14.2% increases in upper neck force and HIC36 values were seen in the Camry seat, while a 19.4% increase in maximum chest displacement was seen in the test bench. A 42.3% increase in maximum pelvis acceleration was seen in the 30MO model with the Camry seat, and a 13.2% increase in maximum head acceleration with the same model and the test bench. The most variation was seen in the 36MO model, with 17.8%, 14.8%, 19.4%, 21.5%, 11.7%, 32.3%, and 19.3% increases in maximum head acceleration, maximum chest displacement, upper neck force, upper neck moment, HIC36, and Nij, respectively. All other metrics showed less than 10% variation between the Camry seat and test bench.

In the rear-facing configuration, the 18MO model and Camry seat showed 17.7%, 58.1%, 25.1%, 11.9%, and 16.5% greater maximum pelvis acceleration, upper neck force, HIC36, head excursion, and Nij, respectively. For the same model, but with the test bench, lower and upper neck moments were 40.0% and 11.4% higher than the model with the Camry seat, respectively. Maximum pelvis acceleration and upper neck moment were 95.6% and 33.6% higher, respectively, in the 24MO model with the Camry seat. Lower neck force and moment, upper neck moment, and head excursion were 11.3%, 61.0%, 32.4%, and 34.3% higher, respectively, in the 24MO model with the test bench. In the 30MO model with the Camry seat, only HIC36 was greater (14.4%), while the lower and upper neck forces, upper neck moment, and Nij were 21.8%, 23.8%, 62.0%, and 44.2% higher, respectively, in the 30MO model with the test bench. Variation was, again, greater in the 36MO model, with lower and upper neck force, lower neck moment, and HIC36 33.9%, 88.2%, 37.5%, and 11.2% larger, respectively, in the model with the Camry seat. Additionally, maximum pelvis acceleration, upper neck moment, and head excursion were 19.3%, 33.3%, and 14.7% greater in the 36MO model with the test bench. All other metrics showed less than 10% variation between the Camry seat and test bench.

Head trajectories varied among seating configurations and ages (Fig. 4). For all four ages, the forward-facing model experienced a longer, wider path. Differences in X position between models in the test bench and Camry seat were relatively small for both seating configurations. The 18MO, 24MO, and 30MO models in the rear-facing configuration, however, experienced differing Z position paths: the models in the Camry seat showed positive Z position throughout the simulations, while the models in the test bench showed negative Z position throughout the simulations (Fig. 4A-C). The Z paths of the 36MO model in the test bench and Camry seat largely differed, with maximum displacements of approximately 220 mm and 40 mm, respectively (Fig. 4D). The largest difference in X displacement between forward-facing and rear-facing was seen in the 18MO model, with maximum displacements of approximately 150 mm and 400 mm, respectively (Fig. 4A).

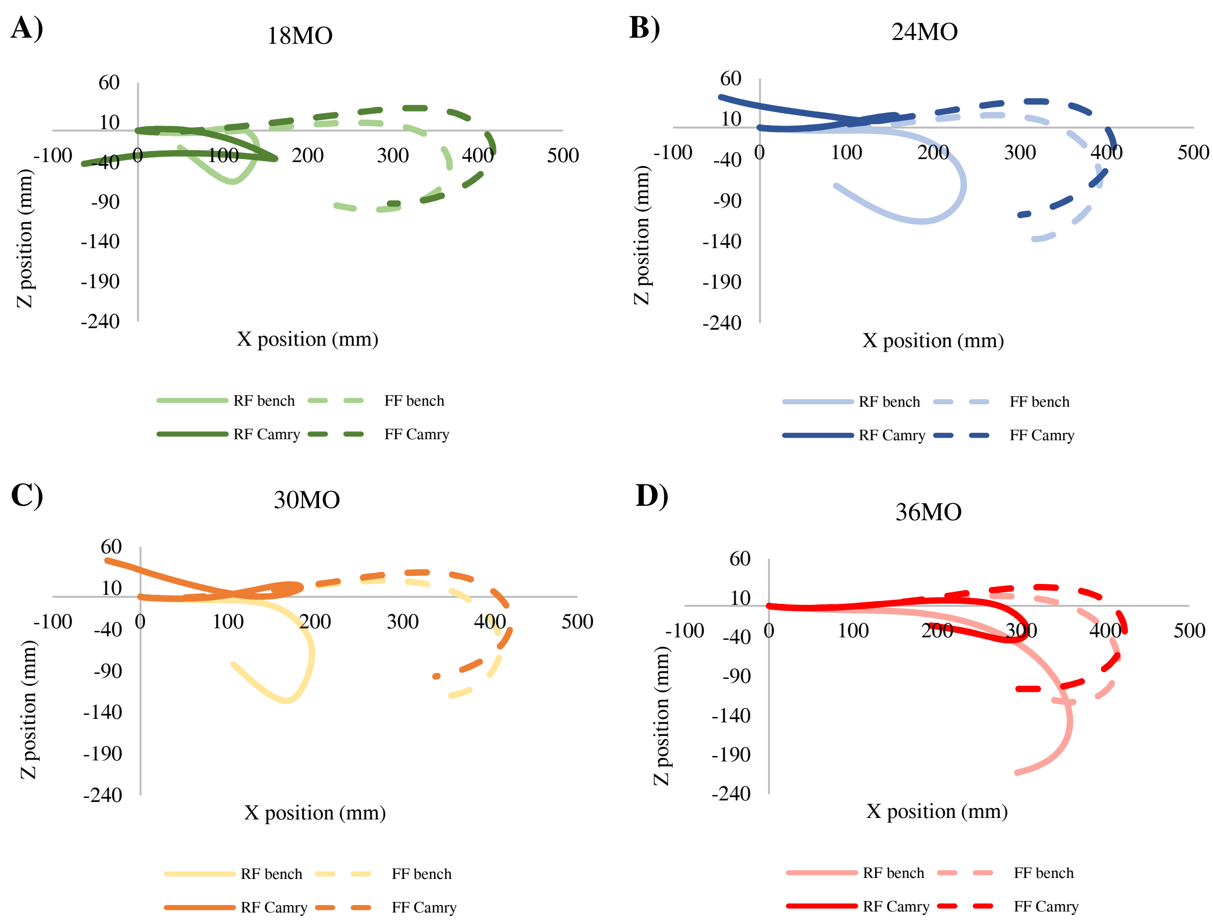

Figure 4. Head trajectories for the A) 18MO (green), B) 24MO (blue), C) 30MO (orange), and D) 36MO (red) during the simulated frontal crash.

DISCUSSION

Head acceleration was relatively similar in forward-facing and rear-facing configurations for all ages, but variation generally increased as age increased. Increased head acceleration was seen in the 36MO model, which may have been due to its higher mass. In the rear-facing configuration, the heavier 36MO model caused increased compression of the CRS into the base, causing the model and CRS to rotate backward at a higher rate with higher head acceleration. Maximum head acceleration occurred at approximately 55 ms for rear-facing, or when the model was restrained against the back of the CRS, and 80 ms for forward-facing, or when the neck reached maximum flexion. Pelvis acceleration did not show a trend with age, as that of the three younger models were higher in rear-facing

compared to the oldest model greatest in forward-facing for those on the test bench, and all but the 24MO had higher pelvis accelerations in forward-facing for those on the Camry seat. This could be due to the model sliding in the CRS after the initiation of the impact. As the load was distributed across the back face of the CRS, some rear-facing models slid back in the CRS and their legs swung back. In forward-facing, the five-point harness restrained the pelvis from any forward motion relative to the rest of the body, but some models slid forward to contact the harness. This space between the CRS and model or buckle and model are not recommended in real life, but was a limitation to the model, as positioning and gravity-settling may have not placed the model in the optimal position for the simulation by creating spaces between the restraints and the models. The maximum pelvis acceleration occurred at around 85-100 ms for the rear-facing configuration, and at around 45-60 ms in the forward-facing configuration, or when the models reached maximum pelvis displacement relative to their starting positions.

Chest displacement were as expected, with forward-facing models having much higher values. In this seating arrangement, the models accelerated forward and compressed against the harness and buckle, causing greater chest deflection than in rear-facing, where the force of the accelerating models was placed on the back of the CRS instead of the harness and buckle.

Lower neck forces were marginally larger in forward-facing models, with the exception of the 18MO model on the test bench. Upper neck forces and both lower and upper neck moments were almost 12, 7, and 2 times greater in forward-facing models, respectively. Forces in the upper neck were far greater than those in the lower neck, but lower neck moments were far greater than those in the upper neck. As the models absorbed energy from the impact, the head and neck whipped forward, causing the lower neck to compress as the upper neck accelerated forward, rotated, compressed, and flexed. As this happened, a large moment was created in the lower neck as the head and upper neck rotated.

HIC36 was greater in all forward-facing models, and corresponds to the increased neck forces and moments of the forward-facing models. Those exhibiting increased head acceleration and extensive neck flexion were more likely to experience a head injury. Similarly, Nij values were at least 5 magnitudes higher in forward-facing models. By the same logic, those with largely greater head accelerations and neck flexion were more likely to receive a neck injury.

Head excursions were approximately doubled or tripled for models in the forward-facing configuration and were generally higher in the younger models. The apparent neck flexion and head rotation in the forward-facing models was likely the reason for largely increased head excursions. Head trajectories followed the same trend, with larger differences in X and Z positions in the younger models (Fig. 4). Along with head acceleration, an increase in model mass likely caused the rear-facing head excursions and trajectories to increase with age. As the mass of the model increased, the compression of the rear-facing CRS into the base increased, causing the model and CRS to increase backwards rotation and head metrics to increase.

In both forward-facing and rear-facing configurations, the 36MO model showed the most variation in injury metrics between simulations with the Camry seat and test bench. Injury metrics were largely inconsistent among seating configurations and ages, with no apparent trends. This could have been due to model and CRS positioning. If the model was not flush against the back of the CRS after gravity settling and the model slid upon impact, then kinematic injury metrics may have been affected. Similarly, if belt routing was not flush against the model or if the pelvis belts slid during the simulation, then results may have been affected for models on either the test bench or Camry seat. Additionally, the test bench is approximately 30 mm shorter in length than the Camry seat, so the CRS partially hung off the test bench, which caused increased compression of the front of the seat in simulations with the forward-facing model and some with the younger rear-facing models. Positioning of the rear-facing models onto the CRS and base was difficult since the legs of the models restricted how close the model and CRS could be to the back of the base. The older models were positioned a relatively far distance from the back of the base and caused the CRS to partially hang off both the test bench and Camry seat. Model positioning was completed in PIPER via lower limb rotation about the hip, knee, or ankle joints. Due to this, the model and CRS were not in the optimal position on the base.

Limitations

Positioning of the rear-facing model was limiting since the joints could only rotate a certain amount before the integrity of the model was compromised. As a result, the CRSs for some models partially hung off the seat so that enough space was available for the legs. For rear-facing models, this created a large gap between the rear-facing CRS seat pan and the back of the base. The elastic modulus of the CRS was increased to 10 MPa to produce simulation stability, so injury metrics are likely not the same as they would be in real life. The simulation setup of the Camry seat lacked a retractor, pretensioner, and load limiter, so the setup may not have been representative of the matched real-world vehicle seat. Additionally, the foam properties of the Camry seat and 213-test bench were not identical and could contribute to differences in responses among the two bases. The objective of this study was to show differences in injury metrics between forward-facing and rear-facing seating arrangements with the same test conditions, so although these limitations created discrepancies between the simulation and real-world conditions, they equally affected results for both seating configurations, and the overall goal was accomplished. The study considered one make and model of CRS and only frontal impacts. Different manufactuers and CRS types (infant, booster) as well as lateral and rear impacts are likely to produce different injury metrics.

CONCLUSIONS

Kinetics and kinematics numbers across the board were within IARV limits. Pediatric models in rear-facing configurations generally had lower injury numbers than those in forward-facing configurations. However, there is no consistent trend seen in injury values as age progresses. This is the first study to conduct a systematic evaluation of the response of children under three years old in forward- and rear-facing seating arrangements in frontal motor vehicle crashes.

REFERENCES

[1] Truong, W. H., Hill, B. W., & Cole, P. A. (2013). “Automobile safety in children: a review of North American evidence and recommendations.” *Journal of the American Academy of Orthopaedic Surgeons, 21*(6), 323-331.

[2] Romano, E. & Kelley-Baker, T. (2015). “Child passengers injured in motor vehicle crashes.” *Journal of Safety Research, 52*, 1-8.

[3] Rafukka, I. A., Sahari, B. B., Nuraini, A. A., & Manohar, A. (2016). “Child Dummy Finite Element Models Development: A Review.” *ARPN Journal of Engineering and Applied Science*, *11*(10), 6649-6656.

[4] Tarrière, C. (1995). “Children are not miniature adults.” *International Research Conference on the Biomechanics of Impact (IRCOBI)*. September 13-15, Brunnen, Switzerland.

[5] Roth, S., Raul, J. S., Ruan, J., & Willinger R. (2007). “Limitation of Scaling Methods in Child Head Finite Element Modelling.” *International Journal of Vehicle Safety, 2*(4), 404–421.

[6] Ramrattan, N. N., Oner, F. C., Boszczyk, B. M., Castelein, R. M., & Heini, P. F. (2012). “Cervical spine injury in the young child.” *European Spine Journal, 21*(11), 2205-2211.

[7] Platzer, P., Jaindl, M., Thalhammer, G., Dittrich, S., Kutscha-Lissberg, F., Vecsei, V., & Gaebler, C. (2007). “Cervical spine injuries in pediatric patients.” *Journal of Trauma and Acute Care Surgery, 62*(2), 389-396.

[8] Gray, H., & Clement, C. (1984). *Gray's Anatomy of the Human Body*. New York, NY: Lea and Febinger.

[9] Decina, L. E., & Lococo, K. H. (2005). “Child restraint system use and misuse in six states.” *Accident Analysis & Prevention, 37*(3), 583–590.

[10] Decina, L. E., & Lococo, K. H. (2007) “Observed LATCH use and misuse characteristics of child restraint systems in seven states.” *Journal of Safety Research, 38*(3), 273–281.

[11] Eby, D. W., & Kostyniuk, L. P. (1999). "A statewide analysis of child safety seat use and misuse in Michigan." *Accident Analysis & Prevention, 31*(5):555–566

[12] Dukehart, J. G., Walker, L., Lococo, K. H., Decina, L. E., & Staplin, L. (2007). "Safe kids checkup events: a national study." *SafeKids Worldwide*, Washington, DC.

[13] O'Neil, J., Daniels, D. M., Talty, J. L., & Bull, M.J. (2009). "Seat belt misuse among children transported in belt-positioning booster seats." *Accident Analysis & Prevention, 41*(3), 425–429.

[14] Ebel, B. E. & Grossman, D. C. (2003). "Crash Proof Kids? An Overview of Current Motor Vehicle Child Occupant Safety Strategies." *Current Problems in Pediatric Adolescent Health Care,* 38-55.

[15] Tai, A., Bilston, L. E., & Brown, J. (2011). "The cumulative effect of multiple forms of minor incorrect use in forward facing child restraints on head injury risk." *International Technical Conference on the Enhanced Safety of Vehicles (ESV).* Paper 11-0118. Washington, DC, June 13-16.

[16] Lesire, P., Cuny, S., Alonzo, F., Tejera, G., & Cataldi, M. (2007). "Misuse of child restraint systems in crash situations – danger and possible consequences." *The Annual Proceedings of the Association for the Advancement of Automotive Medicine, 51*, 207–222.

[17] Weber, K., & Melvin, J. W. (1983). "Injury potential with misused child restraint systems." SAE 831604. Stapp Car Crash Proceedings. Society of Automotive Engineers, Warrendale.

[18] Kapoor, T., Altenhof, W., Snowdon, A., Howard, A., Rasico, J., Zhu, F., & Baggio, D. (2011). "A numerical investigation into the effect of CRS misuse on the injury potential of children in frontal and side impact crashes." *Accident Analysis & Prevention, 43*(4), 1438–1450.

[19] Lalonde, S., Legault, F., & Pedder, J. (2003). "Relative degradation of safety to children when automotive restraint systems are misused." *International Technical Conference on the Enhanced Safety of Vehicles (ESV).* Paper 03-0085. Nagoya, Japan, May 19-22.

[20] Bilston, L. E., Yuen, M., & Brown, J. (2007). "Reconstruction of crashes involving injured child occupants: the risk of serious injuries associated with sub-optimal restraint use may be reduced by better controlling occupant kinematics." *Traffic Injury Prevention, 8*(1), 47–61.

[21] Klinich, K.D., & Manary, M.A. (2015). "Best Practice Recommendations for Protecting Child Occupants." In N. Yoganandan, A. M. Melvin & J. W. Melvin (Eds.), *Accidental Injury: Biomechanics and Prevention* (pp.697-719). New York, NY: Springer.

[22] Henary, B., Sherwood, C. P., Crandall, J. R., Kent, R. W., Vaca, F. E., Arbogast, K. B., & Bull, M. J. (2007). "Car safety seats for children: rear facing for best protection." *Injury Prevention, 13*(6), 398–402.

[23] Snyder, R. G., Schneider, L. W., Owings, C. L., Reynolds, H. M., Golomb, D. H., & Schork, M. A. (1977). "Anthropometry of Infants, Children, and Youths to Age 18 for Product Safety Design." Consumer Product Safety Commission.